Numerical and experimental study of spray coating using air-assisted high pressure atomizers

Q. Ye[1*], B. Shen[2], O. Tiedje[1] and J. Domnick[3]
[1] Fraunhofer Institute for Manufacturing Engineering and Automation
Nobelstr. 12, 70569 Stuttgart, Germany
[2] University Stuttgart, Nobelstr. 12, 70569 Stuttgart, Germany
[3] University of Applied Sciences Esslingen, Kanalstr. 33, 73728 Esslingen, Germany
qiaoyan.ye@ipa.fraunhofer.de, bo.shen@gsame.uni-stuttgart.de, oliver.tiedje@ipa.fraunhofer.de
and Joachim.Domnick@hs-esslingen.de

Abstract

Airless and Air-assisted Airless spray guns are widely used in the spray painting industry. The present contribution summarizes ongoing investigations on the spray painting processes of these two atomizers using real paint material. Atomization processes under airless and air-assisted conditions were experimentally studied by measuring droplet size distributions and droplet velocities using a Spraytec Fraunhofer type particle sizer and Laser-Doppler Anemometry. A computational fluid dynamics code was applied to calculate the flow field and the droplet trajectories. The measured and calculated film thickness distributions on the substrate were compared. The experimental and simulation results provided the necessary information for understanding the painting process using airless and air-assisted systems and for improving the performance of these atomizers.

Introduction

Spray coating processes are characterized by their relatively large paint wastage and high energy consumption. The unavoidable overspray, caused by poor transfer efficiency, has to be removed quickly from the paint booth, in order to preserve the painting quality on the subject surface. The therefore needed conditioned air stream results in intensive energy requirement for the disposal of the overspray. Demands on energy-efficient painting processes, for instance by using improved spray atomizers, are permanently increasing.

It is well known that air spray atomizers, e.g. pneumatic atomizers, can create very fine droplet size distributions, however with low transfer efficiencies (55 %– 65 %) even in ideal conditions. The air-assisted high pressure atomizer, also known as AirCoat or AirMix, is basically a flat jet airless atomizer with additional air flow for improved atomization and homogenization of the spray cone. For instance, the tailing effect at the edge of the spray pattern of the airless atomizer can be improved by using air-assisted atomization. Compared to the well-known air spray painting, the spray transfer efficiency of airless and air assisted atomizers is relatively high, corresponding to a lower overspray.

Experimental studies involving spray painting using airless guns have been performed by Plesniak et al. [1]. They focused their studies mainly on effects of application parameters on the spray transfer efficiency (TE) in painting booths, e.g., paint mass flow rate, gun-to-target distance, gun-to-target angle, etc. There are only few reports about numerical simulations of spray painting using airless and air-assisted guns and even less investigations on the effect of additional air in air-assisted spray gun on the atomization process.

During the last ten years, detailed experimental and numerical investigations of painting processes by using different atomizers, such as high-speed rotary bells with electrostatic support, pneumatic application using coaxial jet type atomizers, as well as powder coating, have been carried out at the Fraunhofer Institute for Manufacturing Engineering and Automation (IPA) [2-5]. The main task of these investigations was to calculate the film thickness distribution and the transfer efficiency (amount of paint reaching the work piece) for a given set of application parameters and boundary conditions.

The present contribution presents experimental and numerical results of investigations on the spray painting using a typical flat jet air-assisted gun. White base-coat material was used. As Phase-Doppler Anemometry (PDA) cannot be applied with real paint due to optical inhomogeneity of the paint material, Fraunhofer diffraction and Laser-Doppler Anemometry have to be applied in combination. Both experimental techniques delivered the necessary boundary conditions for the trajectory calculation of the droplets in the numerical simulations that were performed by means of the commercial CFD solver ANSYS-FLUENT. The calculated film thickness distribution and the TE on the target were compared with experiments for model assessment. Influ-

* Corresponding author: qiaoyan.ye@ipa.fraunhofer.de

ences of the additional air flow in air-assisted mode on the atomization process were studied by comparing droplet size distributions under airless and air-assisted conditions. The experimental and simulation results provided the necessary information for understanding the painting process and for improving the performance of the atomizer.

Experimental investigations

The basic geometry of the air-assisted atomizer used in this study is shown in Fig.1. Pressure atomization as the major process is performed by applying pressures up to 250 bars through a central paint nozzle with elliptical orifice. Air nozzles around the liquid nozzle assist atomization and shaping nozzles deform the spray cone into round jet if required. By switching off air flow in the air cap, the atomizer works as an airless gun. In the present research, an effective orifice diameter of 0.15 mm with a full spray cone angle of ca. 80° was used. In table 1, properties of the paint material, major characteristics of the air-assisted gun, as well as the specific operating conditions investigated are summarized.

Table 1. Experimental parameters

paint material	Base coat: Calcit white
solid fraction	38 %
density (wet)	1.19 g/ml
density (dry)	1.96 g/ml
pressure supply	120-200 bar, corresponding to a paint mass flow rate of 5.53 -7.45 g/s
Assist atomizing air flow	114 l/min
Shaping air flow	13.9 l/min
effective orifice diameter	approx. 0.15 mm
spray angle	approx. 80°
gun-to-target distance	200 mm
booth air velocity	0.3 m/s

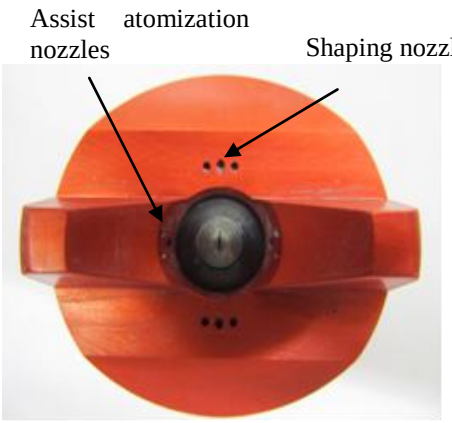

Fig. 1 air nozzles in the air cap of an air-assisted atomizer

LDA measurements

A DANTEC 2-component backscatter fibre LDA system, equipped with a 5 W Ar-ion laser was applied in the present studies, to obtain integral droplet velocities in the spray jet. Figure 2 shows the setup of the LDA measurement. The axial velocity and the velocity component in the direction of the jet spread were measured along the long centre line within the spray cross section 50 mm below the liquid nozzle. Figure 3 shows the measured velocity profiles. It can be seen that the maximum droplet velocity in the spray centre is about 65 m/s for the axial component and 20 m/s for the component in the jet spread direction, respectively, for the air-assisted system with a liquid pressure supply of 200 bar. The measured velocity profiles provide useful information for creating droplet injection file in the following numerical study.

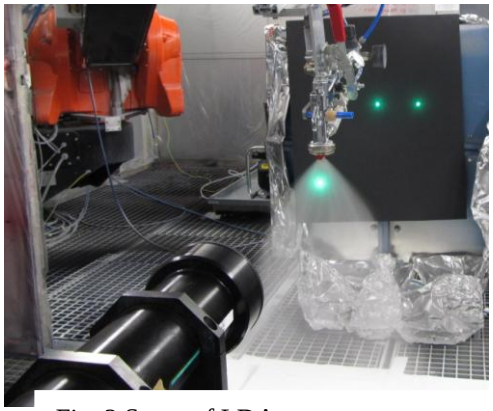

Fig. 2 Setup of LDA measurement

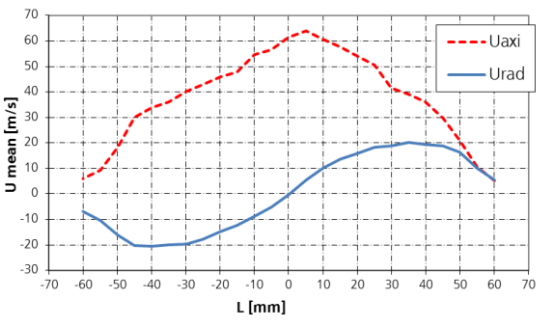

Fig. 3 Measured axial and velocity components in the jet spread direction 50 mm below the liquid nozzle

Droplet size measurement

Droplet size measurements were carried out applying a Malvern Spraytec Fraunhofer type particle sizer at 100 mm distance from the spray nozzle. Since the measuring volume of the laser beam has a diameter of 9 mm, the measured results are actually average values within the tube-shaped measuring volume of the Malvern. Figure 4 shows the setup of the droplet size measurement. By traversing the spray gun that was mounted on a robot along the major axis of the elliptical spray region, droplet size distributions along the major axis of the elliptical spray cone were obtained. In order to allow further comparisons, the droplet distributions created by the airless gun, i. e. without additional air flow, were also measured.

Figure 5 shows the droplet Sauter mean diameter ($D_{3,2}$) distributions in the measured spray cone region at different liquid pressures. Also in the air assist operation mode, flat sprays were created. It can be clearly seen that there is an accumulation of large droplets at both edges of the major axis of the spray pattern for both air-assisted and airless conditions. The difference of Sauter mean diameter between air-assist and airless decreased with increasing pressure supply (200 bar), especially in the spray centre. At the edges of the spray cone droplet Sauter mean diameters produced by airless are significantly large than those from air-assist. The representative droplet size distributions for the measured spray cone, the so-called integral droplet size distributions as shown in Fig. 6 for the pressure supply of 160 bar, were calculated based on the individual size distributions and the measured droplet concentration distributions [5]. The corresponding mean sizes are $D_{3,2}$ = 15.9 µm, $D_{v,50}$ =20.1 µm for airless and $D_{3,2}$ = 13.3 µm, $D_{v,50}$ =17.3 µm for air assist. The integral droplet size distribution is required in the numerical simulations presented below.

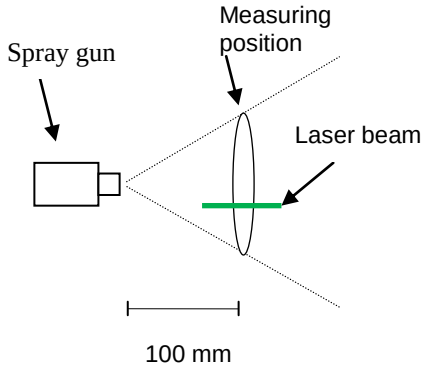

Fig. 4. Setup of droplet size measurement

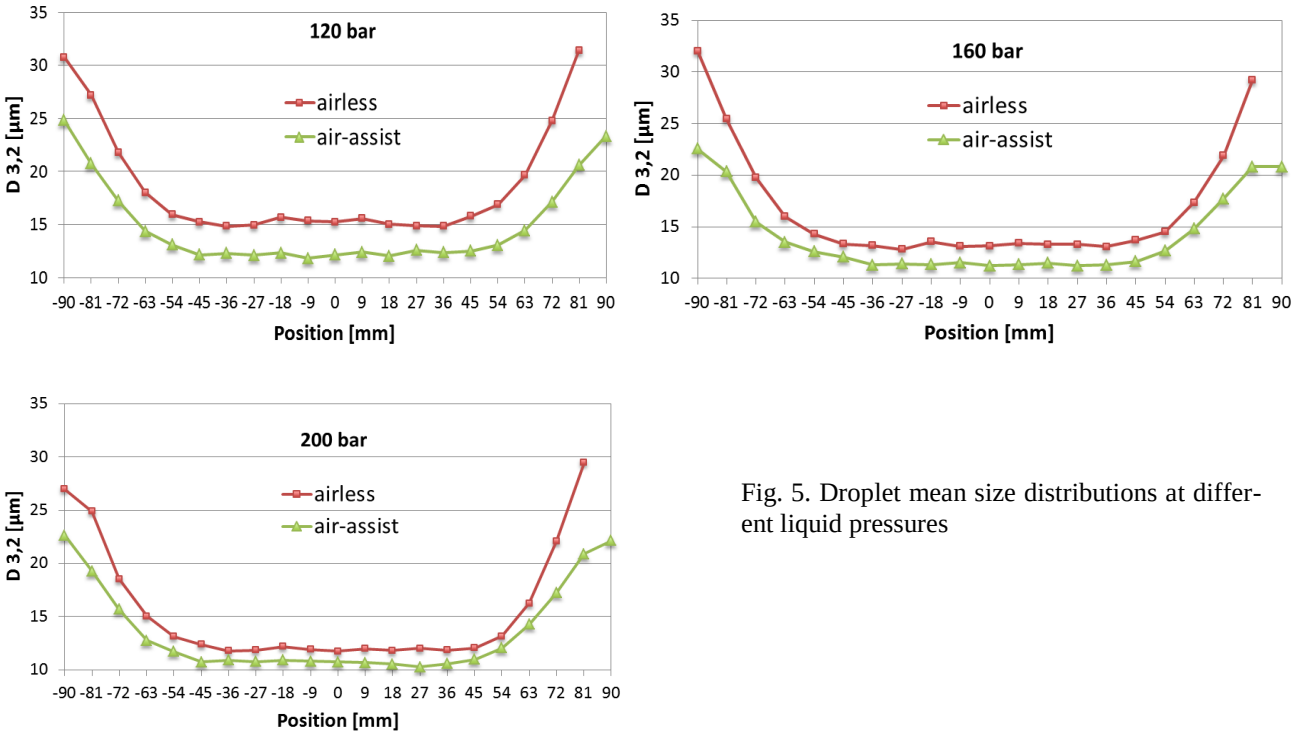

Fig. 5. Droplet mean size distributions at different liquid pressures

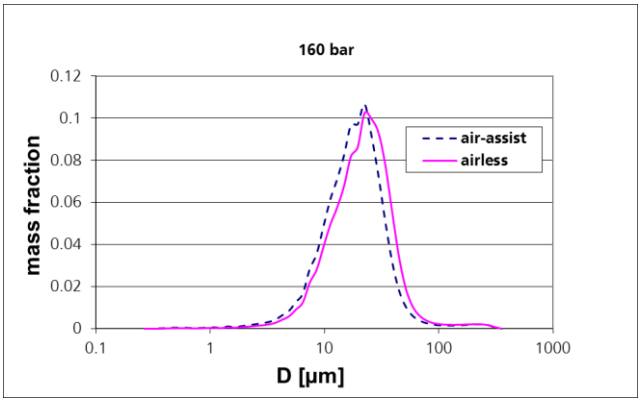

Fig. 6. Integral droplet size distributions for airless and air-assisted system

Paint film thickness measurement

Dynamic spray painting with a relative speed between gun and target of 0.25 m/s and a gun-to-target distance of 200 mm was performed. The target, a flat panel with a size of 200 × 800 mm², was positioned vertically. The gun axis was traversed perpendicular to the target surface so that the major axis of the spray pattern was formed along the 800 mm direction. After painting, the panel was put horizontally into an oven for baking. The dry film thickness on the panel was then measured by means of magneto-inductive method. Figure 7 shows the mean values of the measured film thickness distributions. In case of airless application, the film thickness is characterized by a significant scatter which is, however, further reduced by air-assist. Since the shaping air flow rate was relative low in the present application, there is no significant difference of the width of the spray pattern. The measured transfer efficiency of the paint application was 88% for airless and 78% for air-assisted system.

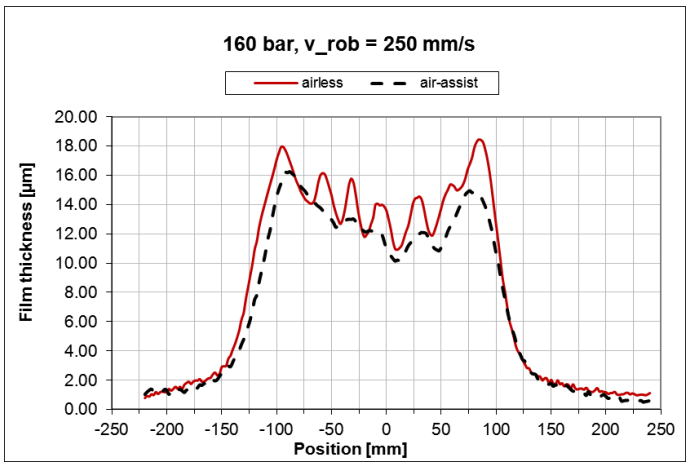

Fig. 7. Dynamic film thickness distributions by airless and air-assisted conditions

Numerical simulation

Computational method

The commercial CFD code ANSYS-FLUENT 14.0, based on the finite-volume approach was applied in the present numerical simulations. The gas phase was modeled using the Eulerian conservation equations for mass and momentum. The three-dimensional incompressible airflow was calculated using couple solver and pseudo-unsteady method. The turbulent transport was modeled using the realizable k-ε model with the scalable standard wall function. An unstructured mesh with 1.5 million cells for the computational domain with a size of 0.6×1.2×0.5 m³ was used.

As primary inlet boundary condition for the continuous phase, a booth air velocity of 0.3 m/s, similar to the experimental condition, and the corresponding mass flow rates of air as given in table 1 for air nozzles were applied. The Lagrangian tracking method was applied for the droplet phase.

Applying numerical simulation to these spray guns a significant problem arises concerning the determination of the inlet conditions for the droplet phase, since the high droplet number density close to the gun anticipates the application of any optic measuring techniques. In previous simulations using a pneumatic atomizer [5] and an airless gun [6] it was found that the initial droplet conditions necessary for the simulation of the liquid phase can be set close to the nozzle. A similar method is applied in the present study. Basically, the droplet injection data was applied to a small rectangular region of 8 × 2 mm², i. e. the projection area of the effective orifice surface, which is considered quite close to the nozzle. As droplet size distribution, the integral distributions created using airless and air-assisted conditions shown in Fig. 6 were applied. Based on the experimental results of the LDA measurements, the axial and the radial velocities of the droplets as well as the droplet flux distribution in the injection region were fitted to match the film thickness distribution on the target panel.

The effect of turbulent dispersion on the particle motion was taken into account by using a stochastic tracking model. The two-way coupling for the momentum exchange between the two phases was applied, which is quite important in the present numerical simulation.

Simulation results

Spray painting simulation was at first carried out under the airless condition, i.e. without additional air flow rate in the atomizer. The booth air velocity of 0.3 m/s was used as the velocity inlet boundary condition in the computational domain. As initial injection conditions, the spray angle of 80° and the droplet axial velocity of 150 m/s were applied. Air velocity contours in a cross-section at x = 0 are depicted in Fig. 8. Velocity contours larger than 30 m/s are blinded out. A higher air velocity can be observed in the spray jet center due to the momentum exchange between the droplet phase and the air phase, especially in the region quite close to the nozzle. The static wet film growth rate on the target is shown in Fig. 9. By artificially moving this spray pattern along the x-direction taking into consideration the robot velocity as well as wet and dry density of the paint material, the dry film thickness distribution on the target was calculated and compared with the experimental results, as shown in Fig. 10. A quite good agreement between experiment and simulation can be observed.

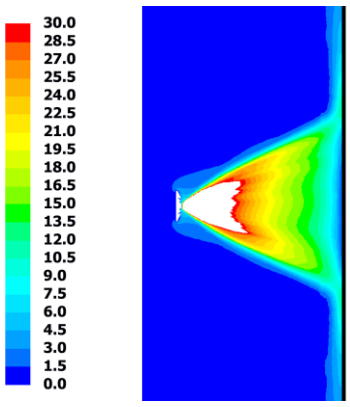

Fig. 8. Velocity contours (m/s) in cross-section x=0 (airless gun)

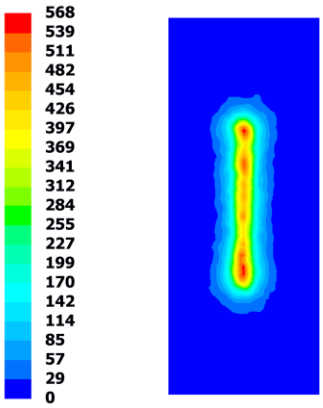

Fig. 9. Calculated static film growth rate on the target (µm/s) (airless gun)

The validated initial injection conditions, for instance, spray angle, droplet velocity as well as liquid flux distribution, were then applied for the spray painting simulation under air-assist case with the assist atomizing air flow rate 114 l/min, shaping air flow rate 13.9 l/min and pressure supply 160 bar for liquid. The corresponding integral droplet size distribution was used. Figure 11 shows the velocity contours close to the atomizer. Significantly higher air velocities due to the assist air nozzles (Fig. 11a) can be observed. The velocities in the shaping air nozzles (Fig. 11b) are relative low, therefore, the flat jet can be still kept. Air velocity contours in a cross-section at x = 0 are shown in Fig.12. Due to the additional air flow rate from the atomizer, the spray jet is narrow than that from the airless model and bimodal velocity contours can be seen. The simulated dynamic film thickness distribution on the flat panel based on the calculated static spray pattern is compared with the corresponding experimental results, as shown in Fig. 13. Again, a reasonably good agreement between experiment and simulation can be observed. The measured and simulated spray transfer efficiencies were 88% and 86%, respectively, for the airless gun, and 78% and 77% for the air-assisted gun. Clearly, the transfer efficiency decreases with increasing assist air flow.

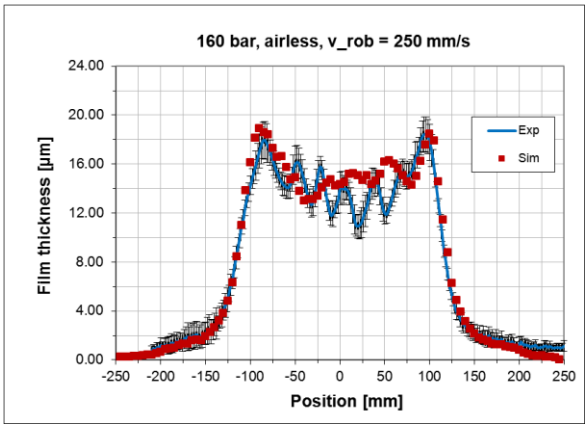

Fig. 10. Comparison of calculated and measured dynamic film thickness distributions (airless)

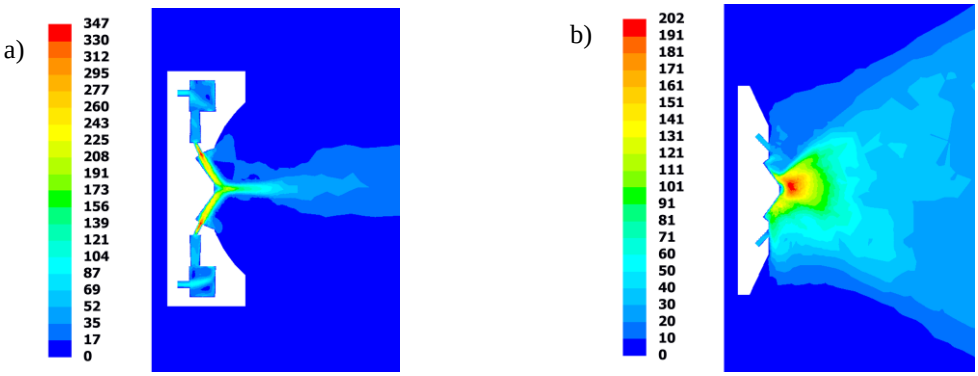

Fig. 11. Velocity contours (m/s) near nozzles (air-assisted gun): a) in cross section y =0, b) in cross section x =0

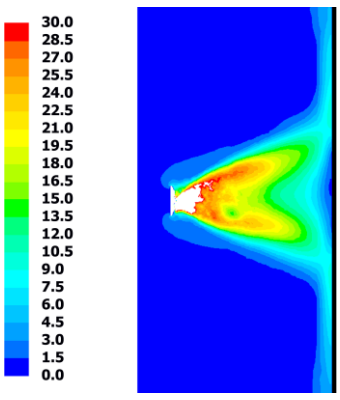

Fig. 12. Velocity contours in cross-section x=0 (air-assisted gun)

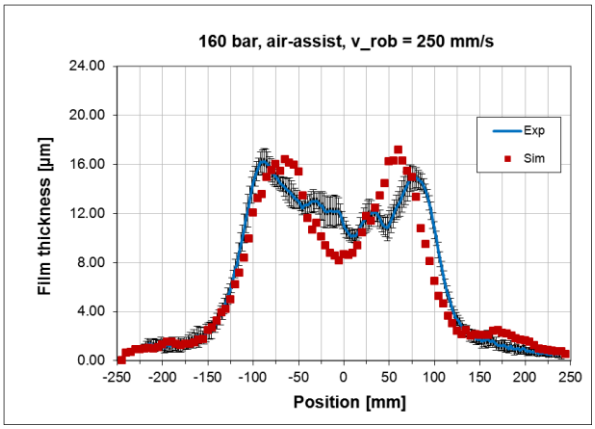

Fig. 13. Comparison of calculated and measured dynamic film thickness distributions (air-assisted gun)

By increasing the shaping air flow rate, 86 l/min, for instance, a narrow spray jet was obtained, as shown in Fig.14. It was found that there were no significant differences in the droplet size distribution. Therefore, the integral droplet size distribution for air-assisted system shown in Fig. 6 could be still used. However, a smaller injection region 4 × 2 mm² close to the liquid nozzle in this case has to be applied. Figure 15 shows the comparison of calculated and measured dynamic film thickness distributions.

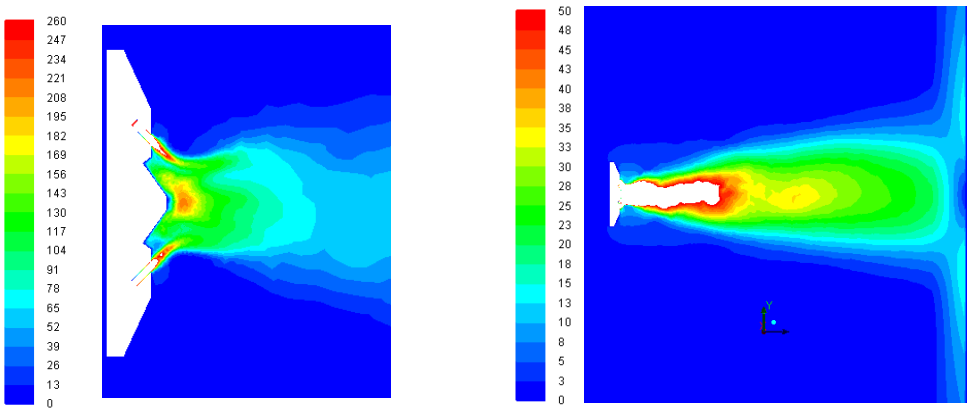

Fig. 14. Velocity contours in cross-section x=0 (air-assisted gun: shaping air flow 86 l/min, assist atomizing air flow 94 l/min). Left: Velocity contours (m/s) near nozzles

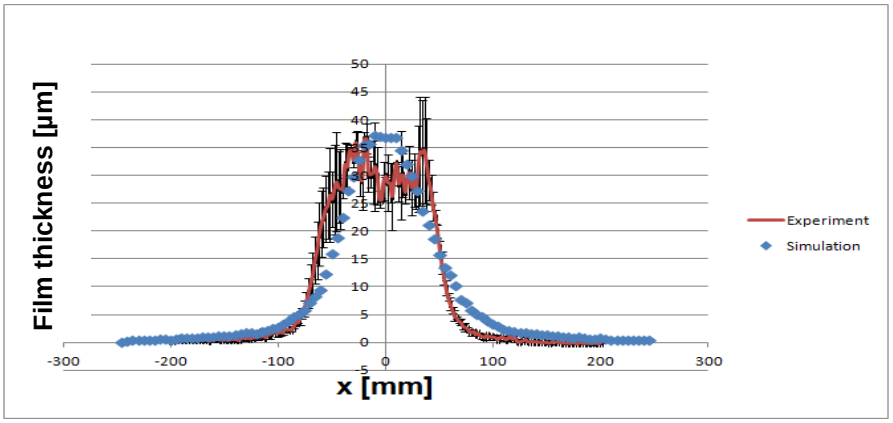

Fig. 15. Comparison of calculated and measured dynamic film thickness distributions (air-assisted gun: shaping air flow 86 l/min, assist atomizing air flow 94 l/min)

Summary and Conclusions

In this paper, experimental and numerical investigations of the spray coating process using an air-assisted gun have been presented.

The atomization processes under airless and air-assist conditions have been experimentally studied by measuring the droplet integral velocity using LDA and by determining the droplet size distributions using a Spraytec Fraunhofer type particle sizer. It was found that the effect of additional atomizing air on the droplet size distribution is diminishing with increasing liquid pressures. Based on the Malvern and the LDA results, the representative integral droplet size distributions were derived.

Based on the experimental results, the injection model for calculating initial conditions of the droplet trajectory simulation was created. Spray painting calculations under airless and air-assist conditions were than carried out with obtained injection data. Model assessment was performed by comparing measured and simulated film thickness distributions.

Based on the present numerical results, further parameter studies will be carried out, aiming to optimize the nozzles in the air cap of the atomizer and to rearrange the air flow rate in the shaping air nozzles, in order to meet the special requirements on paint film thickness distributions in some practical applications. In the wide range of industrial usage (e.g. ships or windmill-powered plants) of airless and air-assisted paint application this

approach will lead to a systematic and scientific optimization in respect of paint consumption and film homogeneity.

References

[1] M. W. Plesniak, P. E. Sojka, A. K. Singh: Transfer Efficiency for Airless Painting Systems, JCT Research, Vol. 1, No. 2, April 2004
[2] Q. Ye, J. Domnick, A. Scheibe: Numerical simulation of spray painting in the automotive industry, Proceedings of the 1st European Automotive CFD Conference Bingen, Germany, June 2003
[3] J. Domnick, A. Scheibe, Q. Ye: The simulation of the electrostatic spray painting process with high-speed rotary bell atomizers. Part I: Direct charging, Part. Part. Syst. Charact. 22 (2005) 141-150
[4] J. Domnick, A. Scheibe, Q. Ye: The simulation of the electrostatic spray painting process with high-speed rotary bell atomizers. Part II: External Charging. Part. Part.Syst. Charact. 23(2006) 408-416
[5] Q.Ye, J. Domnick, E. Khalifa : Simulation of the spray coating process using a pneumatic atomizer. ILASS-Europe, September 2002, Zaragoza
[6] Q. Ye, B. Shen, O. Tiedje, J. Domnick: Investigations of spray painting processes using an airless spray gun. ILASS – Europe 2011, 24th European Conference on Liquid Atomization and Spray Systems, Estoril, Portugal, September 2011